ORGANOMETALLICS

Crystal structure of Fe2Os(CO)12, a structural analog of Fe3(CO)12 with no required site symmetry and only a ~12:1 "star of david" disorder pattern. Example of an acentric, but close to centric, structure. Some thoughts on the solid-state structure of Fe3(CO)12

Melvyn Rowen Churchill, and James C. Fettinger

Organometallics, **1990**, 9 (2), 446-452• DOI: 10.1021/om00116a022 • Publication Date (Web): 01 May 2002

ygen atom of the carboxyl group. By analogy, it is known that tertiary phosphines will add to the CH_2 group of σ–π-coordinated alkenyl groups to form the zwitterionic ligands $R_3P^+CH_2C^-R$, in which the negatively charged carbon atom bridges two metal atoms.[15]

Acknowledgment. These studies were supported by the Office of Basic Energy Sciences of the U.S. Department of Energy (Grant No. DEFG84ER13296).

Supplementary Material Available: Tables of positional parameters for hydrogen atoms and anisotropic thermal parameters for all three crystal structure analyses (10 pages); tables of structure factor amplitudes (55 pages). Ordering information is given on any current masthead page.

---

[15] Churchill, M. R.; DeBoer, B. G.; Shapley, J. R.; Keister, J. B. *J. Am. Chem. Soc.* **1976**, *98*, 2357.

Crystal Structure of $Fe_2Os(CO)_{12}$, a Structural Analogue of $Fe_3(CO)_{12}$ with No Required Site Symmetry and Only a ~12:1 "Star of David" Disorder Pattern: Example of an Acentric, but Close to Centric, Structure. Some Thoughts on the Solid-State Structure of $Fe_3(CO)_{12}$

Melvyn Rowen Churchill* and James C. Fettinger

Department of Chemistry, University at Buffalo, State University of New York, Buffalo, New York 14214

Received July 31, 1989

The heteroatomic trinuclear cluster $Fe_2Os(CO)_{12}$ crystallizes in the noncentrosymmetric monoclinic space group *Pn* (variation of *Pc*; C_s^2; No. 7) with $a = 8.377$ (2) Å, $b = 22.715$ (8) Å, $c = 8.953$ (2) Å, $\beta = 96.510$ (18)°, $V = 1692.6$ (8) $Å^3$, and $Z = 4$. The molecular packing is close to, but not exactly, that required for space group $P2_1/n$ (cf. $Fe_3(CO)_{12}$, $P2_1/n$, $a = 8.359$ (2) Å, $b = 11.309$ (2) Å, $c = 8.862$ (2) Å, $\beta = 97.00$ (2)°, $V = 831.5$ (3) $Å^3$, and $Z = 2$, i.e., similar except that, in the $Fe_2Os(CO)_{12}$ structure, 2_1 and i operations are absent and b is doubled). Diffraction data for $\pm h,+k,\pm l$ were collected for $2\theta = 4.5$–$50.0°$ with Mo Kα radiation. The structure was solved by Patterson and difference-Fourier methods, and refinement converged with $R_F = 4.9\%$, $R_{wF} = 4.8\%$, and GOF = 1.772 for all 5993 point-group-unique reflections ($R_F = 4.0\%$, $R_{wF} = 4.6\%$ for those 5220 data with $|F_o| > 6\sigma(|F_o|)$). There are two crystallographically distinct $Fe_2Os(CO)_{12}$ molecules in the unit cell. Each suffers an approximately 12:1 "star of David" disorder of the metal atoms. The major components are unambiguously defined and contain an $Os(CO)_4$ system linked to two $Fe(CO)_3$ units, which, in turn, are bridged by two asymmetrically bridging carbonyl ligands—i.e., a connectivity similar to that in $Fe_3(CO)_{12}$. Bond lengths of note (in Å) are as follows: molecule A, Os(A)–Fe(1A) = 2.735 (2), Os(A)–Fe(2A) = 2.740 (3), Fe(1A)–Fe(2A) = 2.589 (4), Fe(1A)–C(BR1A) = 2.245 (16), Fe(2A)–C(BR1A) = 1.939 (16), Fe(1A)–C(BR2A) = 1.918 (17), Fe(2A)–C(BR2A) = 2.224 (16); molecule B, Os(B)–Fe(1B) = 2.745 (3), Os(B)–Fe(2B) = 2.746 (3), Fe(1B)–Fe(2B) = 2.594 (4), Fe(1B)–C(BR1B) = 2.084 (20), Fe(2B)–C(BR1B) = 2.047 (19), Fe(1B)–C(BR2B) = 1.937 (17), Fe(2B)–C(BR2B) = 2.123 (17).

Introduction

The saga of the structural characterization of triiron dodecacarbonyl, $Fe_3(CO)_{12}$, has been vividly recounted by Wei and Dahl.[1] Further refinement of the crystal structure was later carried out by Cotton and Troup.[2] It is established that *in the macroscopic solid state* the molecule has structure 1 and that the molecules are statistically disordered about sites of $\bar{1}$ (C_i) symmetry in space group $P2_1/n$.

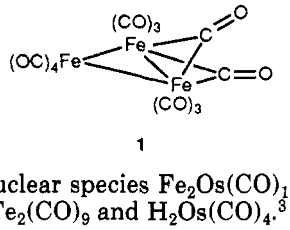

1

The heteronuclear species $Fe_2Os(CO)_{12}$ has been synthesized from $Fe_2(CO)_9$ and $H_2Os(CO)_4$.[3] The substitutional reactivity of this material has recently been studied by Shojaie and Atwood.[4] As a prelude to investigating some products of substitution, we have carried out a single-crystal X-ray diffraction study on the parent compound, $Fe_2Os(CO)_{12}$. Our results, reported below, may also have relevance toward understanding the crystal structure of $Fe_3(CO)_{12}$.

Experimental Section

Collection of X-ray Diffraction Data for $Fe_2Os(CO)_{12}$. Crystals were provided by Shojaie and Atwood.[4] A black crystal with approximate dimensions 0.30 × 0.30 × 0.33 mm was inserted into a glass capillary with its extended direction parallel to the wall of the capillary. It was then mounted in a eucentric goniometer and accurately aligned and centered on a Syntex $P2_1$ automated four-circle diffractometer. All further setup operations (i.e. determination of the crystal's unit cell parameters and orientation matrix) and collection of the intensity data were performed as described previously.[5] Details appear in Table I. The

---

[1] Wei, C. H.; Dahl, L. F. *J. Am. Chem. Soc.* **1969**, *91*, 1351. See also: Desiderato, R., Jr.; Dobson, G. R. *J. Chem. Educ.* **1982**, *59*, 752.

[2] Cotton, F. A.; Troup, J. M. *J. Am. Chem. Soc.* **1974**, *96*, 4155.

[3] Graham, A. R.; Moss, J. R. *J. Organomet. Chem.* **1970**, *23*, C23.

[4] Shojaie, R.; Atwood, J. D. *Inorg. Chem.* **1988**, *27*, 2558.

0276-7333/90/2309-0446$02.50/0

Table I. Experimental Data for the X-ray Diffraction Study of $Fe_2Os(CO)_{10}(\mu\text{-}CO)_2$

(A) Unit Cell Data

cryst syst: monoclinic	space group: *Pn*
a = 8.377 (2) Å	Z = 4
b = 22.715 (8) Å	formula: $C_{12}O_{12}Fe_2Os$
c = 8.953 (2) Å	mol wt: 638.03
β = 96.510 (18)°	D(calcd) = 2.50 g/cm^3
V = 1692.6 (8) Å^3	T = 24 °C (297 K)

(B) Collection of X-ray Diffraction Data

diffractometer: Syntex $P2_1$
radiation: Mo K$\bar{\alpha}$ ($\bar{\lambda}$ = 0.710 730 Å)
monochromator: highly oriented (pyrolytic) graphite; equatorial mode with 2θ(m) = 12.160°; assumed to be 50% perfect/50% ideally mosaic for polarizn cor
rflns measd: $\pm h,+k,\pm l$ for 2θ = 4.5–50.0°, yielding 5993 point-group-unique data
scan type: coupled θ(cryst)–2θ(counter)
scan width: [2θ(Kα_1) – 0.8]–[2θ(Kα_2) + 0.8]°
scan speed: 4.0°/min (2θ)
bkgds: stationary cryst, stationary counter at the two extremes of the 2θ scan; each for $^1/_4$ of the total scan time
std rflns: 3 mutually orthogonal rflns collected before each set of 97 data points; no decay obsd
abs cor: μ(Mo K$\bar{\alpha}$) = 97.3 cm^{-1}, corrected empirically by interpolation (in 2θ and ϕ) between 6 close-to-axial (ψ-scan) rflns; rflns used were 162 (2θ = 15.30°, T_{min}/T_{max} = 0.693), 282 (20.20°, 0.699), 392 (24.43°, 0.728), 2,11,3 (26.72°, 0.718), 3,11,3 (29.22°, 0.744), and 4,12,3 (33.50°, 0.771)

Table II. Intensity Statistics for $Fe_2Os(CO)_{10}(\mu\text{-}CO)_2$

function	obsd	ideal	
		acentric	centric
$\langle\lvert E\rvert\rangle$	0.873	0.886	0.798
$\langle\lvert E\rvert^2\rangle$	1.000	1.000	1.000
$\langle\lvert E\rvert^2 - 1\rangle$	0.747	0.736	0.968
$\lvert E\rvert$ > 1.0, %	36.72	36.79	31.73
$\lvert E\rvert$ > 1.2, %	23.36	23.69	23.01
$\lvert E\rvert$ > 1.4, %	13.79	14.09	16.15
$\lvert E\rvert$ > 1.6, %	7.94	7.73	10.96
$\lvert E\rvert$ > 1.8, %	4.05	3.92	7.19
$\lvert E\rvert$ > 2.0, %	2.33	1.89	4.55
$\lvert E\rvert$ > 2.5, %	0.37	0.19	1.24
$\lvert E\rvert$ > 3.0, %	0.03	0.01	0.27

final cell parameters are based upon a least-squares analysis of the setting angles (2θ, ω, χ) of 25 automatically centered reflections, well dispersed in reciprocal space, with 2θ = 20–30° (Mo K$\bar{\alpha}$ radiation).

The crystal was found to exhibit the systematic absences $h0l$ for $h + l = 2n + 1$, consistent with either the centrosymmetric monoclinic space group $P2/n$ (a nonstandard setting of $P2/c$; C_{2h}^4; No. 13, having the equipoints $\pm(x, y, z; {}^1/_2 + x, \bar{y}, {}^1/_2 + z)$) or the noncentrosymmetric space group Pn (a nonstandard setting of Pc; C_s^2; No. 7, having the equipoints $x, y, z; {}^1/_2 + x, \bar{y}, {}^1/_2 + z$). Data were therefore collected for the octants $\pm h,+k,\pm l$. This provides two equivalent forms for space group $P2/n$ ($+h,+k,+l = -h,+k,-l$ and $-h,+k,+l = +h,+k,-l$) or a single point-group-unique form for space group Pn (thereby allowing the determination of crystal polarity via anomalous dispersion). The completed structural analysis revealed that the true space group is the noncentrosymmetric Pn. (See Table II for intensity statistics, which are uniformly indicative of the acentric case.)

Solution and Refinement of the Structure. All crystallographic calculations were performed on a Syntex XTL system, which incorporated the use of the SUNY—Buffalo modified-version of the XTL interactive crystallographic program package.

The analytical form of the scattering factor for the appropriate neutral atoms[6a] was used in calculating F_c values; corrections were made for both the real ($\Delta f'$) and imaginary ($\Delta f''$) components of anomalous dispersion.[6b]

Table III. Final Atomic Parameters for $Fe_2Os(CO)_{12}$

atom	x	y	z	B(iso), Å^2
		Molecule A		
Os(A)	0.00000 (0)	–0.13493 (3)	0.00000 (0)	
Os(A′)	0.0965 (20)	–0.11341 (47)	0.3374 (19)	4.62 (25)
Fe(1A)	0.22549 (31)	–0.13714 (11)	0.24599 (26)	
Fe(2A)	–0.05702 (29)	–0.09640 (13)	0.27907 (28)	
Fe(1A′)	0.1580 (21)	–0.15860 (83)	0.0659 (19)	0.79 (28)
Fe(2A′)	–0.1090 (30)	–0.1046 (11)	0.0869 (28)	2.88 (47)
C(1A)	–0.2126 (23)	–0.13030 (65)	–0.1154 (21)	4.33 (33)
C(2A)	0.1250 (21)	–0.15977 (72)	–0.1575 (21)	4.31 (33)
C(3A)	0.0449 (16)	–0.05296 (62)	–0.0386 (16)	2.95 (26)
C(4A)	–0.0364 (21)	–0.21778 (83)	0.0595 (20)	4.29 (35)
C(11A)	0.3596 (20)	–0.12474 (66)	0.4171 (19)	4.37 (30)
C(12A)	0.3404 (21)	–0.09781 (73)	0.1155 (19)	4.24 (33)
C(13A)	0.2957 (19)	–0.20828 (72)	0.1971 (18)	4.19 (30)
C(21A)	–0.0792 (21)	–0.08091 (71)	0.4747 (20)	4.34 (33)
C(22A)	–0.1657 (20)	–0.03552 (75)	0.2015 (19)	4.55 (32)
C(23A)	–0.2207 (22)	–0.14544 (82)	0.2445 (20)	4.74 (36)
C(BR1A)	0.1324 (18)	–0.04684 (67)	0.2899 (17)	3.37 (29)
C(BR2A)	0.0752 (20)	–0.17784 (66)	0.3554 (20)	3.87 (29)
O(1A)	–0.3295 (18)	–0.13025 (56)	–0.1823 (20)	
O(2A)	0.1921 (22)	–0.17091 (76)	–0.2496 (18)	
O(3A)	0.0722 (16)	–0.00574 (52)	–0.0688 (15)	
O(4A)	–0.0618 (18)	–0.26381 (52)	0.0792 (16)	
O(11A)	0.4540 (20)	–0.11667 (52)	0.5197 (17)	
O(12A)	0.4267 (18)	–0.07401 (65)	0.0503 (18)	
O(13A)	0.3433 (19)	–0.25435 (62)	0.1748 (17)	
O(21A)	–0.0922 (20)	–0.07080 (69)	0.5991 (15)	
O(22A)	–0.2342 (20)	0.00645 (72)	0.1599 (17)	
O(23A)	–0.3318 (18)	–0.17801 (65)	0.2451 (19)	
O(BR1A)	0.1888 (15)	–0.00306 (54)	0.3012 (15)	
O(BR2A)	0.0485 (17)	–0.21933 (59)	0.4213 (15)	
		Molecule B		
Os(B)	–0.41083 (9)	–0.38736 (3)	–0.15249 (7)	
Os(B′)	–0.5281 (12)	–0.36324 (37)	–0.4867 (13)	2.89 (20)
Fe(1B)	–0.65092 (31)	–0.37452 (12)	–0.38559 (30)	
Fe(2B)	–0.35689 (31)	–0.35676 (12)	–0.43921 (29)	
Fe(1B′)	–0.5715 (29)	–0.3855 (11)	–0.1926 (27)	2.74 (44)
Fe(2B′)	–0.2781 (29)	–0.3824 (12)	–0.2540 (27)	2.77 (42)
C(1B)	–0.3922 (19)	–0.46780 (72)	–0.2098 (17)	3.65 (29)
C(2B)	–0.4286 (19)	–0.30233 (72)	–0.1087 (17)	3.84 (32)
C(3B)	–0.1981 (23)	–0.39117 (68)	–0.0467 (22)	4.62 (35)
C(4B)	–0.5382 (21)	–0.40487 (79)	0.0093 (22)	4.70 (36)
C(11B)	–0.7984 (19)	–0.36307 (64)	–0.5477 (18)	4.13 (29)
C(12B)	–0.7595 (25)	–0.33443 (87)	–0.2523 (23)	5.35 (40)
C(13B)	–0.7190 (21)	–0.44675 (80)	–0.3371 (20)	4.95 (35)
C(21B)	–0.3439 (19)	–0.33584 (71)	–0.6338 (19)	3.92 (32)
C(22B)	–0.2391 (22)	–0.29676 (84)	–0.3572 (21)	5.31 (39)
C(23B)	–0.1929 (23)	–0.40941 (83)	–0.4234 (20)	4.68 (35)
C(BR1B)	–0.5050 (24)	–0.42563 (76)	–0.5078 (23)	4.88 (34)
C(BR2B)	–0.5539 (20)	–0.29928 (75)	–0.4228 (19)	4.27 (32)
O(1B)	–0.3806 (17)	–0.51696 (50)	–0.2406 (16)	
O(2B)	–0.4424 (16)	–0.25561 (48)	–0.0873 (13)	
O(3B)	–0.0726 (18)	–0.39435 (59)	0.0222 (19)	
O(4B)	–0.6128 (21)	–0.41759 (83)	0.1060 (17)	
O(11B)	–0.8919 (18)	–0.35451 (55)	–0.6428 (18)	
O(12B)	–0.8300 (18)	–0.31039 (63)	–0.1763 (19)	
O(13B)	–0.7655 (18)	–0.49216 (65)	–0.3092 (20)	
O(21B)	–0.3222 (20)	–0.32549 (75)	–0.7447 (15)	
O(22B)	–0.1575 (22)	–0.25814 (73)	–0.3160 (18)	
O(23B)	–0.0951 (19)	–0.44471 (74)	–0.4187 (23)	
O(BR1B)	–0.5122 (18)	–0.46721 (58)	–0.5817 (14)	
O(BR2B)	–0.5703 (18)	–0.24882 (56)	–0.4455 (16)	

The structure was solved by the successful location of two independent osmium atoms from a Patterson map in space group Pn with Z = 4; two independent molecules therefore define the asymmetric unit. Least-squares refinement (three cycles full matrix) led to R_F = 29.3% and R_{wF} = 35.2%.[7] A difference-Fourier synthesis was now performed, yielding the positions of the four iron atoms. Three cycles of full-matrix least-squares refinement led to R_F = 15.2%, R_{wF} = 19.8%. Subsequent difference-Fourier syntheses led to the location of all atoms of the carbonyl groups (R_F = 7.4%). At this point a further difference-Fourier synthesis was performed. Six independent peaks

---

(5) Churchill, M. R.; Lashewycz, R. A.; Rotella, F. J. *Inorg. Chem.* **1977**, *16*, 265.

(6) (a) *International Tables for X-ray Crystallography*; Kynoch Press: Birmingham, England, 1974; Vol IV, pp 99–101. (b) *Ibid.*, pp 149–150.

(7) R_F (%) = $100[(\sum\lvert\lvert F_o\rvert - \lvert F_c\rvert\rvert)/\sum\lvert F_o\rvert]$; R_{wF} (%) = $100[(\sum w(\lvert F_o\rvert - \lvert F_c\rvert)^2)/\sum w\lvert F_o\rvert^2]^{1/2}$, where $1/w = [\sigma(\lvert F_o\rvert)]^2 + [0.015\lvert F_o\rvert]^2$; GOF = $[\sum w(\lvert F_o\rvert - \lvert F_c\rvert)^2/(\mathrm{NO} - \mathrm{NV})]^{1/2}$, where NO = number of observations and NV = number of variables.

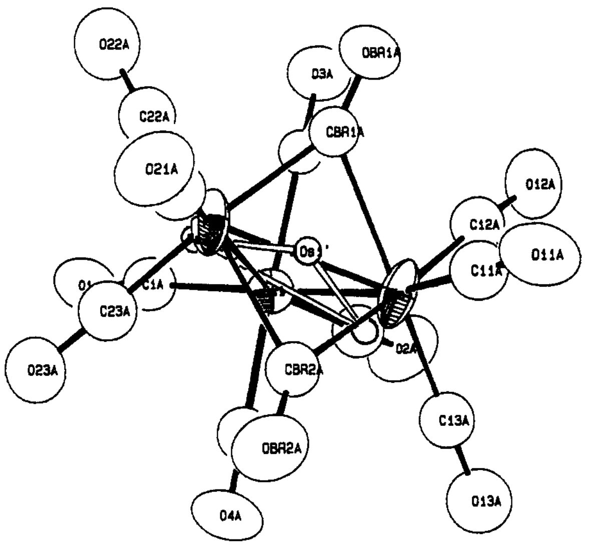

Figure 1. ORTEP-II diagram for molecule A of $Fe_2Os(CO)_{10}(\mu\text{-}CO)_2$. The *b* direction is vertical, and *a* is horizontal. The minor-component atoms are artificially reduced.

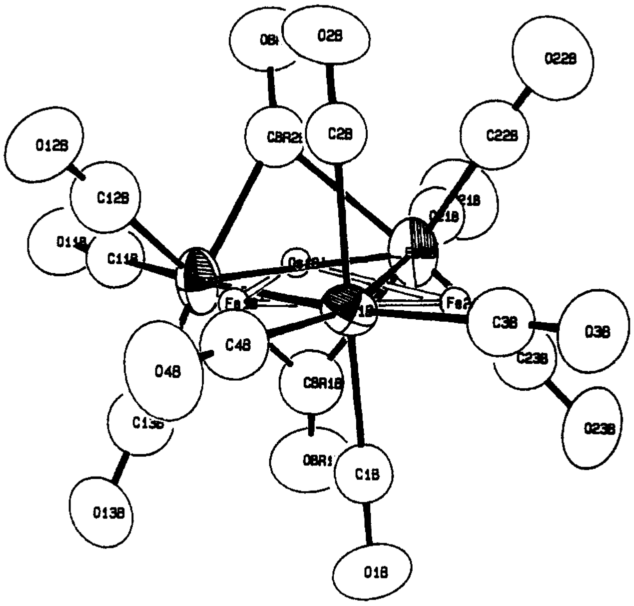

Figure 2. ORTEP-II diagram for molecule B of $Fe_2Os(CO)_{10}(\mu\text{-}CO)_2$, with *b* vertical and *a* horizontal (i.e., the same as for Figure 1). This is the molecule related to molecule A by a pseudo inversion center. Note that the major Fe_2Os core is tipped from the horizontal by a lesser degree than that in Figure 1.

Table IV. Interatomic Distances (Å) for $Fe_2Os(CO)_{12}$

molecule A		molecule B	
(A) Metal–Metal Distances (Major Components)			
Os(A)–Fe(1A)	2.735 (2)	Os(B)–Fe(1B)	2.745 (3)
Os(A)–Fe(2A)	2.740 (3)	Os(B)–Fe(2B)	2.746 (3)
Fe(1A)–Fe(2A)	2.589 (4)	Fe(1B)–Fe(2B)	2.594 (4)
(B) Metal–Metal Distances (Minor Components)			
Os(A′)–Fe(1A′)	2.740 (24)	Os(B′)–Fe(1B′)	2.745 (27)
Os(A′)–Fe(2A′)	2.675 (30)	Os(B′)–Fe(2B′)	2.815 (27)
Fe(1A′)–Fe(2A′)	2.576 (31)	Fe(1B′)–Fe(2B′)	2.580 (34)
(C) Metal–Carbon Distances (Major Components)			
Os(A)–C(1A)	1.958 (19)	Os(B)–C(1B)	1.909 (16)
Os(A)–C(2A)	1.933 (18)	Os(B)–C(2B)	1.980 (16)
Os(A)–C(3A)	1.938 (14)	Os(B)–C(3B)	1.923 (20)
Os(A)–C(4A)	1.989 (19)	Os(B)–C(4B)	1.935 (19)
Fe(1A)–C(11A)	1.816 (17)	Fe(1B)–C(11B)	1.815 (16)
Fe(1A)–C(12A)	1.828 (17)	Fe(1B)–C(12B)	1.824 (21)
Fe(1A)–C(13A)	1.791 (17)	Fe(1B)–C(13B)	1.806 (18)
Fe(1A)–C(BR1A)	2.245 (16)	Fe(1B)–C(BR1B)	2.084 (20)
Fe(1A)–C(BR2A)	1.918 (17)	Fe(1B)–C(BR2B)	1.937 (17)
Fe(2A)–C(21A)	1.816 (18)	Fe(2B)–C(21B)	1.820 (17)
Fe(2A)–C(22A)	1.755 (17)	Fe(2B)–C(22B)	1.790 (19)
Fe(2A)–C(23A)	1.766 (19)	Fe(2B)–C(23B)	1.815 (19)
Fe(2A)–C(BR1A)	1.939 (16)	Fe(2B)–C(BR1B)	2.047 (19)
Fe(2A)–C(BR2A)	2.224 (16)	Fe(2B)–C(BR2B)	2.123 (17)
(D) Metal–Carbon Distances (Minor Components)			
Os(A′)–C(11A)	2.252 (24)	Os(B′)–C(11B)	2.268 (19)
Os(A′)–C(21A)	2.153 (24)	Os(B′)–C(21B)	2.228 (20)
Os(A′)–C(BR1A)	1.608 (19)	Os(B′)–C(BR1B)	1.446 (19)
Os(A′)–C(BR2A)	1.485 (19)	Os(B′)–C(BR2B)	1.585 (19)
Fe(1A′)–C(2A)	1.988 (26)	Fe(1B′)–C(2B)	2.315 (30)
Fe(1A′)–C(4A)	2.107 (26)	Fe(1B′)–C(4B)	1.850 (32)
Fe(1A′)–C(12A)	2.070 (25)	Fe(1B′)–C(12B)	1.980 (32)
Fe(1A′)–C(13A)	1.917 (24)	Fe(1B′)–C(13B)	2.185 (31)
Fe(1A′)–···C(3A)	2.707 (23)	Fe(1B′)···C(1B)	2.414 (30)
Fe(2A′)–C(1A)	2.005 (31)	Fe(2B′)–C(1B)	2.218 (32)
Fe(2A′)–C(3A)	2.151 (29)	Fe(2B′)–C(3B)	1.911 (31)
Fe(2A′)–C(22A)	1.961 (30)	Fe(2B′)–C(22B)	2.194 (33)
Fe(2A′)–C(23A)	2.006 (31)	Fe(2B′)–C(23B)	1.852 (31)
Fe(2A′)···C(4A)	2.661 (31)	Fe(2B′)···C(2B)	2.639 (31)
(E) Carbon–Oxygen Distances			
C(1A)–O(1A)	1.089 (25)	C(1B)–O(1B)	1.157 (20)
C(2A)–O(2A)	1.079 (25)	C(2B)–O(2B)	1.087 (20)
C(3A)–O(3A)	1.136 (18)	C(3B)–O(3B)	1.159 (25)
C(4A)–O(4A)	1.086 (22)	C(4B)–O(4B)	1.160 (25)
C(11A)–O(11A)	1.157 (23)	C(11B)–O(11B)	1.107 (23)
C(12A)–O(12A)	1.119 (23)	C(12B)–O(12B)	1.096 (26)
C(13A)–O(13A)	1.146 (22)	C(13B)–O(13B)	1.140 (24)
C(21A)–O(21A)	1.155 (22)	C(21B)–O(21B)	1.056 (22)
C(22A)–O(22A)	1.152 (24)	C(22B)–O(22B)	1.147 (26)
C(23A)–O(23A)	1.190 (24)	C(23B)–O(23B)	1.143 (25)
C(BR1A)–O(BR1A)	1.101 (20)	C(BR1B)–O(BR1B)	1.151 (23)
C(BR2A)–O(BR2A)	1.147 (21)	C(BR2B)–O(BR2B)	1.170 (21)

with heights of up to ~6 e/Å^3 indicated that the structure possessed some form of disorder. These peaks were found to lie in the planes of the three metal atoms in each of the two independent molecules. Within each molecule, the three metal atoms and three residual peaks formed a "star of David" pattern indicative of disorder involving either (i) a 180° rotational disorder of a major and minor molecular orientation or (ii) an inversion disorder of the major and minor molecular orientation. Since the independent molecule has C_2 (and approximate C_{2v}) symmetry, these alternatives are indistinguishable in the present case. The secondary osmium atoms were distinguished from iron atoms on the basis of (a) peak heights on the difference-Fourier map and (b) interatomic distances (Os–Fe > Fe–Fe).

Careful refinement of the occupancies of the major and minor components yielded average normalized values of 0.925 and 0.075 (an approximately 12:1 ratio). Inversion of coordinates, with appropriate changes in B_{12} and B_{23} values, now gave lower R_F and R_{wF} values; the crystal polarity was thus redefined at this stage of the analysis. Two cycles of refinement gave the residuals R_F = 5.1% and R_{wF} = 5.0%. An extinction correction was now performed; the correction applied was very small, with $g = 1.245 \times 10^{-7}$ in the expression $|F_{o,corr}| = |F_{o,uncorr}|(1.0 + gI_o)$. Convergence of the model was achieved with the major components of the metal atoms and the oxygen atoms assigned anisotropic thermal parameters and all other atoms having isotropic thermal parameters. The residuals for all 5993 reflections were R_F = 4.9%, R_{wF} = 4.8%, and GOF = 1.772. These were reduced to R_F = 4.3%, R_{wF} = 4.7%, and GOF = 1.813 for those 5585 reflections with $|F_o| > 3\sigma(|F_o|)$ and to R_F = 4.0%, R_{wF} = 4.6%, and GOF = 1.841 for those 5220 reflections with $|F_o| > 6\sigma(|F_o|)$. A final difference-Fourier synthesis was now performed, revealing only peaks of height <1 e/Å^3.

If we assume that the disorder pattern follows that of $Fe_3(CO)_{12}$,[1] our model omits secondary carbon atoms (and, possibly, secondary oxygen sites[2]) of occupancy 0.075. This would correspond to "pseudoatoms" containing 0.45 e (0.075 × C) and 0.60 e (0.075 × O). We feel justified in this omission.

Final atomic positions are listed in Table III. (Anisotropic thermal parameters appear as supplementary material.)

Description of the Crystal Structure of $Fe_2Os(CO)_{12}$

Crystals are composed of discrete molecular units of composition $Fe_2Os(CO)_{10}(\mu\text{-}CO)_2$. There are two crystallographically independent units in the asymmetric unit. The labeling of molecule A is shown in Figure 1; that of molecule B is shown in Figure 2. Interatomic distances and angles are compiled in Tables IV and V, respectively.

Each of the molecular sites is subject to a 0.925:0.075 (~12:1) disorder, with the same "star of David" pattern of disorder for the Fe_2Os cores as is observed in $Fe_3(CO)_{12}$.[1,2] However, for $Fe_2Os(CO)_{10}(\mu\text{-}CO)_2$, the molecules are in general positions and the connectivity of the major components can be observed directly. Crystalline $Fe_3(CO)_{12}$ contains units of $Fe_3(CO)_{10}(\mu\text{-}CO)_2$ that are statistically disordered about sites of C_i ($\bar{1}$) symmetry, and elucidation of the *molecular* geometry must be inferred.[1,2] Here, the two Fe_3 units form a "star of David" pattern with a required 0.5:0.5 occupancy about crystal-averaged inversion centers. Further comparisons of the *crystal structures* of $Fe_2Os(CO)_{10}(\mu\text{-}CO)_2$ and $Fe_3(CO)_{10}(\mu\text{-}CO)_2$ will be deferred to later.

We now come to the details of the molecular geometry of $Fe_2Os(CO)_{10}(\mu\text{-}CO)_2$. Parameters for both the major and minor components are available in Tables IV and V. Within the text we will describe the geometry of the major components only. In molecule A, metal–metal distances are Os(A)–Fe(1A) = 2.735 (2) Å, Os(A)–Fe(2A) = 2.740 (3) Å, and Fe(1A)–Fe(2A) = 2.589 (4) Å; in molecule B, Os(B)–Fe(1B) = 2.745 (3) Å, Os(B)–Fe(2B) = 2.746 (3) Å, and Fe(1B)–Fe(2B) = 2.594 (4) Å. Average metal–metal bond lengths are Os–Fe = 2.742 ± 0.005 Å and Fe–Fe = 2.592 ± 0.004 Å. (The comparable dibridged Fe–Fe distance in $Fe_3(CO)_{10}(\mu\text{-}CO)_2$ is 2.558 (1) Å, while the nonbridged distances are 2.677 (2) and 2.683 (1) Å; the dibridged Fe–Fe linkage in $Fe_3(CO)_{10}(\mu\text{-}CO)_2$ being shorter than that in $Fe_2Os(CO)_{10}(\mu\text{-}CO)_2$ probably is a geometric result of shorter nonbridged Fe–Fe, vis à vis Os–Fe, linkages.)

Osmium–carbonyl distances range from 1.909 (16) through 1.989 (19) Å, averaging 1.943 Å; the precision of the structural determination is not sufficient to enable us to distinguish between axial and equatorial Os–CO distances (cf. Os–CO(axial) = 1.946 ± 0.006 Å vs Os–CO(equatorial) = 1.912 ± 0.007 Å in $Os_3(CO)_{12}$).[8] Terminal iron–carbonyl distances range from 1.755 (17) through 1.828 (17) Å, averaging 1.804 Å (cf. Fe–CO(average) = 1.82 Å in $Fe_3(CO)_{10}(\mu\text{-}CO)_2$).[2] Terminal C–O distances are 1.056 (22)–1.190 (24) Å (average 1.134 Å).

We now come to the $Fe(\mu\text{-}CO)_2Fe$ bridges within the two $Fe_2Os(CO)_{10}(\mu\text{-}CO)_2$ molecules. In molecule A, the short Fe(1A)–C(BR2A) bond is counterbalanced by the long Fe(2A)–C(BR2A) interaction (1.918 (17) vs 2.224 (16) Å) and the short Fe(2A)–C(BR1A) bond is counterbalanced by the long Fe(1A)–C(BR1A) interaction (1.939 (16) vs 2.245 (16) Å); the differences of 0.306 and 0.306 Å are identical, and the idealized total molecular symmetry of C_2 (as determined for $Fe_3(CO)_{10}(\mu\text{-}CO)_2$[1,2]) is confirmed. Appropriate M–C–O angles are Fe(1A)–C(BR2A)–O(BR2A) = 146.7 (14)° vs Fe(2A)–C(BR2A)–O(BR2A) = 136.2 (14)° and Fe(2A)–C(BR1A)–O(BR1A) = 150.4 (14)° vs Fe(1A)–C(BR1A)–O(BR1A) = 133.4 (13)°.

Unfortunately, the situation for molecule B is not quite so clear-cut. Thus, we have Fe(1B)–C(BR2B) = 1.937 (17) Å vs Fe(2B)–C(BR2B) = 2.123 (17) Å and Fe(2B)–C(BR1B) = 2.047 (19) Å vs Fe(1B)–C(BR1B) = 2.084 (20) Å—i.e., lesser asymmetries of 0.186 and 0.037 Å only. The most probable explanation of this is that the energy profile from the asymmetrically bridging case to the symmetrically bridging case is very flat and is in the same energetic range as weak intermolecular forces.

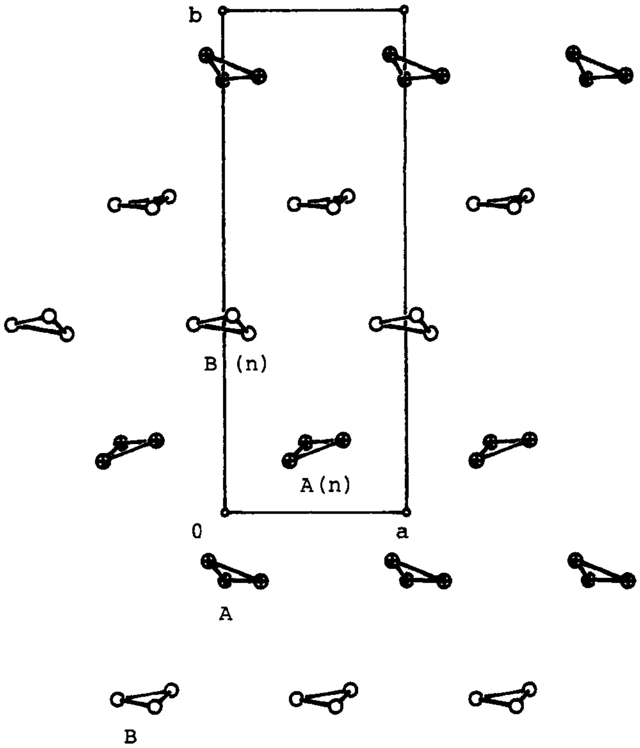

Figure 3. Positioning of the Fe_2Os units (major components only) in the packing of $Fe_2Os(CO)_{10}(\mu\text{-}CO)_2$. Type A molecules are shaded. The basic unit cell is outlined (*b* vertical, *a* horizontal). The *n*-glide planes are at $y = 0, {}^1/_2, 1$.

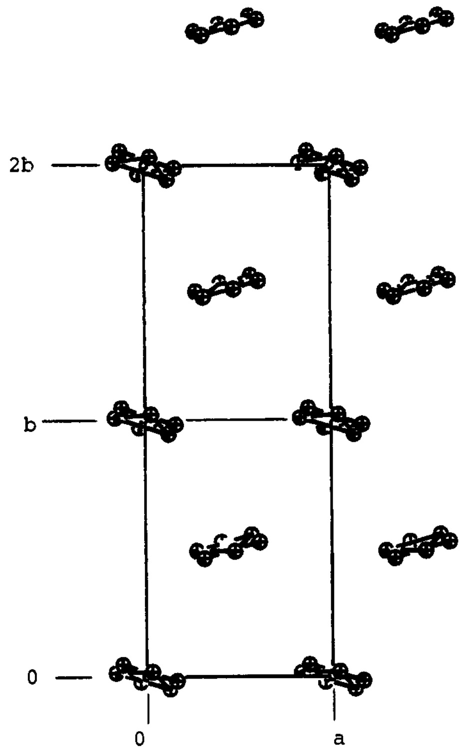

Figure 4. Positioning of Fe_3 units in the packing of disordered $Fe_3(CO)_{10}(\mu\text{-}CO)_2$. The double unit cell 2*b* (vertical) and *a* (horizontal) is outlined. The *n*-glide planes are at $y = {}^1/_4, {}^3/_4, {}^5/_4, {}^7/_4$; the 2_1 axes lie along *y* at $x = {}^1/_4, {}^3/_4$ and $z = 0, {}^1/_2, 1$; inversion centers are at $x = 0, {}^1/_2, 1$, $y = 0, {}^1/_2, 1, 1{}^1/_2, 2$, and $z = 0, {}^1/_2, 1$.

---

(8) Churchill, M. R.; DeBoer, B. G. *Inorg. Chem.* 1977, *16*, 878.

Table V. Interatomic Angles (deg) for $Fe_2Os(CO)_{12}$

molecule A		molecule B	
(A) Metal–Metal–Metal Angles (Major Components)			
Fe(1A)–Os(A)–Fe(2A)	56.45 (8)	Fe(1B)–Os(B)–Fe(2B)	56.39 (8)
Os(A)–Fe(1A)–Fe(2A)	61.88 (8)	Os(B)–Fe(1B)–Fe(2B)	61.83 (8)
Os(A)–Fe(2A)–Fe(1A)	61.67 (8)	Os(B)–Fe(2B)–Fe(1B)	61.79 (8)
(B) Metal–Metal–Metal Angles (Minor Components)			
Fe(1A′)–Os(A′)–Fe(2A′)	56.81 (72)	Fe(1B′)–Os(B′)–Fe(2B′)	55.28 (76)
Os(A′)–Fe(1A′)–Fe(2A′)	60.33 (75)	Os(B′)–Fe(1B′)–Fe(2B′)	63.74 (83)
Os(A′)–Fe(2A′)–Fe(1A′)	62.86 (77)	Os(B′)–Fe(2B′)–Fe(1B′)	60.99 (81)
(C) Metal–Metal–Carbon Angles (Major Components)			
Fe(1A)–Os(A)–C(1A)	158.4 (5)	Fe(1B)–Os(B)–C(1B)	88.4 (5)
Fe(1A)–Os(A)–C(2A)	101.6 (5)	Fe(1B)–Os(B)–C(2B)	89.0 (5)
Fe(1A)–Os(A)–C(3A)	91.8 (4)	Fe(1B)–Os(B)–C(3B)	159.7 (6)
Fe(1A)–Os(A)–C(4A)	83.1 (5)	Fe(1B)–Os(B)–C(4B)	99.9 (6)
Fe(2A)–Os(A)–C(1A)	102.8 (5)	Fe(2B)–Os(B)–C(1B)	87.9 (5)
Fe(2A)–Os(A)–C(2A)	157.4 (5)	Fe(2B)–Os(B)–C(2B)	87.8 (5)
Fe(2A)–Os(A)–C(3A)	85.0 (4)	Fe(2B)–Os(B)–C(3B)	103.3 (6)
Fe(2A)–Os(A)–C(4A)	90.6 (5)	Fe(2B)–Os(B)–C(4B)	156.2 (6)
Os(A)–Fe(1A)–C(11A)	168.9 (5)	Os(B)–Fe(1B)–C(11B)	175.5 (5)
Os(A)–Fe(1A)–C(12A)	80.9 (5)	Os(B)–Fe(1B)–C(12B)	86.1 (7)
Os(A)–Fe(1A)–C(13A)	92.0 (5)	Os(B)–Fe(1B)–C(13B)	86.8 (6)
Os(A)–Fe(1A)–C(BR1A)	84.4 (4)	Os(B)–Fe(1B)–C(BR1B)	85.2 (5)
Os(A)–Fe(1A)–C(BR2A)	89.2 (5)	Os(B)–Fe(1B)–C(BR2B)	86.5 (5)
Fe(2A)–Fe(1A)–C(11A)	109.5 (5)	Fe(2B)–Fe(1B)–C(11B)	113.9 (5)
Fe(2A)–Fe(1A)–C(12A)	116.9 (6)	Fe(2B)–Fe(1B)–C(12B)	126.7 (7)
Fe(2A)–Fe(1A)–C(13A)	132.9 (5)	Fe(2B)–Fe(1B)–C(13B)	121.2 (6)
Fe(2A)–Fe(1A)–C(BR1A)	46.6 (4)	Fe(2B)–Fe(1B)–C(BR1B)	50.5 (5)
Fe(2A)–Fe(1A)–C(BR2A)	56.8 (5)	Fe(2B)–Fe(1B)–C(BR2B)	53.5 (5)
Os(A)–Fe(2A)–C(21A)	171.3 (6)	Os(B)–Fe(2B)–C(21B)	174.0 (5)
Os(A)–Fe(2A)–C(22A)	91.6 (6)	Os(B)–Fe(2B)–C(22B)	87.2 (6)
Os(A)–Fe(2A)–C(23A)	81.4 (6)	Os(B)–Fe(2B)–C(23B)	87.9 (6)
Os(A)–Fe(2A)–C(BR1A)	90.3 (5)	Os(B)–Fe(2B)–C(BR1B)	85.9 (6)
Os(A)–Fe(2A)–C(BR2A)	83.3 (4)	Os(B)–Fe(2B)–C(BR2B)	83.1 (5)
Fe(1A)–Fe(2A)–C(21A)	112.0 (6)	Fe(1B)–Fe(2B)–C(21B)	112.2 (5)
Fe(1A)–Fe(2A)–C(22A)	132.6 (6)	Fe(1B)–Fe(2B)–C(22B)	122.2 (6)
Fe(1A)–Fe(2A)–C(23A)	117.1 (6)	Fe(1B)–Fe(2B)–C(23B)	127.6 (6)
Fe(1A)–Fe(2A)–C(BR1A)	57.3 (5)	Fe(1B)–Fe(2B)–C(BR1B)	51.8 (6)
Fe(1A)–Fe(2A)–C(BR2A)	46.2 (4)	Fe(1B)–Fe(2B)–C(BR2B)	47.2 (5)
(D) Carbon–Metal–Carbon Angles			
C(1A)–Os(A)–C(2A)	99.6 (7)	C(1B)–Os(B)–C(2B)	175.7 (7)
C(1A)–Os(A)–C(3A)	92.2 (7)	C(1B)–Os(B)–C(3B)	89.4 (7)
C(1A)–Os(A)–C(4A)	92.0 (7)	C(1B)–Os(B)–C(4B)	94.2 (7)
C(2A)–Os(A)–C(3A)	91.1 (7)	C(2B)–Os(B)–C(3B)	91.9 (7)
C(2A)–Os(A)–C(4A)	91.8 (7)	C(2B)–Os(B)–C(4B)	89.6 (7)
C(3A)–Os(A)–C(4A)	174.6 (7)	C(3B)–Os(B)–C(4B)	100.4 (8)
C(11A)–Fe(1A)–C(12A)	98.2 (8)	C(11B)–Fe(1B)–C(12B)	96.1 (8)
C(11A)–Fe(1A)–C(13A)	99.1 (7)	C(11B)–Fe(1B)–C(13B)	96.8 (8)
C(11A)–Fe(1A)–C(BR1A)	84.5 (7)	C(11B)–Fe(1B)–C(BR1B)	92.7 (7)
C(11A)–Fe(1A)–C(BR2A)	91.3 (7)	C(11B)–Fe(1B)–C(BR2B)	89.8 (7)
C(12A)–Fe(1A)–C(13A)	94.2 (8)	C(12B)–E(1B)–C(13B)	95.8 (9)
C(12A)–Fe(1A)–C(BR1A)	83.3 (7)	C(12B)–Fe(1B)–C(BR1B)	170.9 (9)
C(12A)–Fe(1A)–C(BR2A)	170.1 (7)	C(12B)–Fe(1B)–C(BR2B)	85.5 (8)
C(13A)–Fe(1A)–C(BR1A)	176.0 (7)	C(13B)–Fe(1B)–C(BR1B)	80.8 (8)
C(13A)–Fe(1A)–C(BR2A)	86.7 (7)	C(13B)–Fe(1B)–C(BR2B)	173.1 (8)
C(BR1A)–Fe(1A)–C(BR2A)	95.1 (6)	C(BR1B)–Fe(1B)–C(BR2B)	96.8 (7)
C(21A)–Fe(2A)–C(22A)	97.1 (8)	C(21B)–Fe(2B)–C(22B)	96.0 (8)
C(21A)–Fe(2A)–C(23A)	97.4 (8)	C(21B)–Fe(2B)–C(23B)	96.9 (8)
C(21A)–Fe(2A)–C(BR1A)	90.7 (7)	C(21B)–Fe(2B)–C(BR1B)	90.7 (8)
C(21A)–Fe(2A)–C(BR2A)	88.1 (7)	C(21B)–Fe(2B)–C(BR2B)	92.1 (7)
C(22A)–Fe(2A)–C(23A)	94.0 (8)	C(22B)–Fe(2B)–C(23B)	95.3 (9)
C(22A)–Fe(2A)–C(BR1A)	87.0 (7)	C(22B)–Fe(2B)–C(BR1B)	172.6 (8)
C(22A)–Fe(2A)–C(BR2A)	174.3 (7)	C(22B)–Fe(2B)–C(BR2B)	84.3 (8)
C(23A)–Fe(2A)–C(BR1A)	171.7 (8)	C(23B)–Fe(2B)–C(BR1B)	87.0 (8)
C(23A)–Fe(2A)–C(BR2A)	83.0 (7)	C(23B)–Fe(2B)–C(BR2B)	171.0 (8)
C(BR1A)–Fe(2A)–C(BR2A)	95.2 (6)	C(BR1B)–Fe(2B)–C(BR2B)	92.4 (7)
(E) Metal–Carbon–Oxygen Angles (Major Components)			
Os(A)–C(1A)–O(1A)	176.7 (17)	Os(B)–C(1B)–O(1B)	178.2 (14)
Os(A)–C(2A)–O(2A)	176.1 (17)	Os(B)–C(2B)–O(2B)	178.0 (15)
Os(A)–C(3A)–O(3A)	176.4 (13)	Os(B)–C(3B)–O(3B)	177.2 (16)
Os(A)–C(4A)–O(4A)	173.7 (17)	Os(B)–C(4B)–O(4B)	177.4 (17)
Fe(1A)–C(11A)–O(11A)	175.1 (15)	Fe(1B)–C(11B)–O(11B)	176.9 (15)
Fe(1A)–C(12A)–O(12A)	171.0 (16)	Fe(1B)–C(12B)–O(12B)	177.2 (19)

Table V (Continued)

molecule A		molecule B	
(E) Metal–Carbon–Oxygen Angles (Major Components)			
Fe(1A)–C(13A)–O(13A)	175.9 (15)	Fe(1B)–C(13B)–O(13B)	178.2 (17)
Fe(1A)–C(BR1A)–O(BR1A)	133.4 (13)	Fe(1B)–C(BR1B)–O(BR1B)	139.8 (16)
Fe(1A)–C(BR2A)–O(BR2A)	146.7 (14)	Fe(1B)–C(BR2B)–O(BR2B)	148.3 (15)
Fe(2A)–C(21A)–O(21A)	179.4 (16)	Fe(2B)–C(21B)–O(21B)	173.2 (17)
Fe(2A)–C(22A)–O(22A)	175.2 (16)	Fe(2B)–C(22B)–O(22B)	174.1 (18)
Fe(2A)–C(23A)–O(23A)	169.6 (17)	Fe(2B)–C(23B)–O(23B)	176.0 (18)
Fe(2A)–C(BR1A)–O(BR1A)	150.4 (14)	Fe(2B)–C(BR1B)–O(BR1B)	142.2 (16)
Fe(2A)–C(BR2A)–O(BR2A)	136.2 (14)	Fe(2B)–C(BR2B)–O(BR2B)	131.9 (14)
(F) Metal–(μ-C)–Metal Angles			
Fe(1A)–C(BR1A)–Fe(2A)	76.1 (5)	Fe(1B)–C(BR1B)–Fe(2B)	77.8 (7)
Fe(1A)–C(BR2A)–Fe(2A)	77.0 (6)	Fe(1B)–C(BR2B)–Fe(2B)	79.3 (6)

Unit Cells of $Fe_2Os(CO)_{10}(\mu\text{-}CO)_2$ and $Fe_3(CO)_{10}(\mu\text{-}CO)_2$

The unit cell dimensions of the Fe_2Os complex are a = 8.377 (2) Å, b = 22.715 (8) Å, c = 8.953 (2) Å, and β = 96.510 (18)°; those for the Fe_3 complex are[2] a = 8.359 (2) Å, b = 11.309 (2) Å, c = 8.862 (2) Å, and β = 97.00 (2)°. The exact ratios (Fe_2Os:Fe_3) are 1.002:1 for a, 2.009:1 for b, 1.010:1 for c, and 0.995:1 for β. This correspondence led us to hope that we might be able to determine whether there could be any microscopic order as opposed to macroscopic disorder in the crystal structure of $Fe_3(CO)_{10}(\mu\text{-}CO)_2$.

Figures 3 and 4 show the orientations of Fe_2Os and Fe_3 triangles in $Fe_2Os(CO)_{10}(\mu\text{-}CO)_2$ and $Fe_3(CO)_{10}(\mu\text{-}CO)_2$.

Let us first consider the crystal packing of $Fe_2Os(CO)_{10}(\mu\text{-}CO)_2$ in detail. As is clearly shown in Figure 3, there are four orientations of molecules, arranged in layers, up the b axis. These are labeled as follows (starting from the bottom of the figure): B (molecule B, whose coordinates are listed in Table III), A (molecule A from Table III), A(n) (related to molecule A by an n glide at y = 0), and B(n) (related to molecule B by an n glide at y = 0); this pattern then repeats by virture of a b translation.

We solved this structure in the noncentrosymmetric space group Pn, rather than its potential centrosymmetric supergroup $P2/n$. This choice is clearly correct—there is, indeed, only one orientation of molecules at any one level along the b axis. (In space group $P2/n$, there must be a 2-fold axis about b, two molecular orientations in each layer, and only two such layers in the cell.) Nevertheless, the structure has definite indications of having *approximate* (but not exact) inversion centers. (Note that the x and z coordinates are not specifically determined in space group Pn; we defined an origin by fixing x = 0 and z = 0 for Os(1A).) Molecule A is related to molecule B by an approximate inversion center at x = –0.2084, y = –0.2478, z = –0.0754. The metal atoms, taken in pairs, yield averaged coordinates as follows: Os(A) + Os(B), x = –0.2054, y = –0.2611, z = –0.0763; Fe(1A) + Fe(1B), x = –0.2127, y = –0.2558, z = –0.0698; Fe(2A) + Fe(2B), x = –0.2070, y = –0.2266, z = –0.0801. The correspondence between the lighter atoms (whose positions are, in essence, dictated by the orientations of the metal clusters) is not so precise. Thus, the coordinates O(BR1A) + O(BR1B) average to x = –0.16165, y = –0.2351, z = –0.1403 and O(BR2A) + O(BR2B) average to x = –0.2610, y = –0.2341, z = –0.0121.

Note that, if the inversion center is precise and is at y = $-^1/_4$, then all four molecules are interrelated by symmetry elements: A → B (inversion center at y = $-^1/_4$), A → A(n) (n glide at y = 0), and A → B(n) (2_1 axis); in this case, the space group will then be the centrosymmetric $P2_1/n$. (Cell dimensions are unchanged, and a standard set of coordinates can be obtained by moving the inversion center to 0, 0, 0 from ~–0.2084, $-^1/_4$ (required), ~–0.0754.)

Table VI. 0*k*0 Data for $Fe_2Os(CO)_{10}(\mu\text{-}CO)_2$ ($|F_o|$, $\sigma(|F_o|)$, $|F_c|$ ×10)

rfln *hkl*	$|F_o|$ ($\sigma(|F_o|)$)	$|F_c|$	rfln *hkl*	$|F_o|$ ($\sigma(|F_o|)$)	$|F_c|$
030	102 (10)	66	0,16,0	834 (15)	857
040	4260 (64)	4074	0,17,0	645 (13)	658
050	207 (11)	300	0,18,0	138 (26)	130
060	0 (27)	27	0,19,0	606 (13)	609
070	655 (11)	660	0,20,0	43 (56)	62
080	3337 (50)	3172	0,21,0	510 (13)	516
090	603 (12)	635	0,22,0	0 (40)	87
0,10,0	0 (30)	44	0,23,0	800 (16)	798
0,11,0	489 (10)	517	0,24,0	0 (31)	20
0,12,0	1159 (18)	1203	0,25,0	339 (17)	402
0,13,0	982 (16)	969	0,26,0	138 (32)	82
0,14,0	0 (25)	37	0,27,0	379 (18)	392
0,15,0	940 (16)	928			

The alert reader will now wonder why we have not made this transformation in order (a) to correctly define the structure and (b) to avoid being "Marshed".[9] The answer is simple. The *raw data* negate this possibility. We have taken the liberty of reproducing our 0*k*0 data in Table VI. Here it can clearly be seen that we do *not* have the required systematic absences 0*k*0 for $k = 2n + 1$ necessary for a crystallographically precise 2_1 axis along b. The profiles for the 0($2n$ + 1)0 reflections are normal—i.e., similar to all other data. Furthermore, the final agreement between $|F_o|$ and $|F_c|$ for this group of reflections is excellent! (An interesting, but unrelated, observation is that 0*k*0 reflections with $k = 4n$ are intense and those with $k = 4n + 2$ are very weak; this, of course, results from the four almost equally spaced and close-to-parallel layers of metal atoms along b giving rise to constructive and destructive interference, respectively, for these two groups of reflections.)

Thus, the structure of $OsFe_2(CO)_{10}(\mu\text{-}CO)_2$ is correctly described in space group Pn but is *close* to the related supergroup $P2_1/n$. (Overall intensity statistics also predict the acentric case (vide supra).)

We now come to the crystal structure of $Fe_3(CO)_{10}(\mu\text{-}CO)_2$ (Figure 4). The macroscopic structure has been treated as a disordered ensemble in space group $P2_1/n$.[1,2] This structure has two distinct layers of molecules up the b axis. Arranged about the origin are the three atoms of the defined Fe_3 cluster; superposed on these is the inversion-related Fe_3 cluster, forming an overall "star of David" pattern. The second layer is centered about $^1/_2$, $^1/_2$, $^1/_2$ and contains mutually opposed triangular Fe_3 units related (by an n-glide plane and a 2_1 axis) to the defined Fe_3 cluster. The contents of the double cell (a, $2b$, c) is the

---

(9) This is a colloquialism heard recently and based upon Dr. R. E. Marsh's publications in which previously published structures are corrected by the inclusion of further elements of symmetry. See, for example: Marsh, R. E. *Organometallics* **1989**, *8*, 1583.

same as that for the idealized ($P2_1/n$) cell of $Fe_2Os(CO)_{10}(\mu\text{-}CO)_2$ (after a change of origin (vide supra)), except that each Fe_3 unit is 0.50:0.50 disordered, whereas the Fe_2Os units are only 0.925:0.075 disordered. The observed $Fe_3(CO)_{10}(\mu\text{-}CO)_2$ structure can arise by two routes.

(1) As described by Wei and Dahl,[1] the exterior of the molecule (an icosahedron of O atoms) may be invariant to inversion of the molecule. In this case, each site may be occupied, on a statistical basis, by "normal" and "inverted" $Fe_3(CO)_{10}(\mu\text{-}CO)_2$ molecules. However, Cotton and Troup[2] found not only two sites for each carbon atom but also *two sites for each oxygen atom.* This indicates that the 12 exterior oxygen atoms of the "normal" and "inverted" molecules do not overlap precisely and that the polyhedron defined by the 12 oxygen atoms does not possess a perfect inversion center. This brings us to a second possible model, based upon the $Fe_2Os(CO)_{10}(\mu\text{-}CO)_2$ structure.

(2) The microscopic packing of $Fe_3(CO)_{10}(\mu\text{-}CO)_2$ molecules could be based on the double cell *a*, 2*b*, *c* in which the individual sites are ordered. A perfectly ordered domain is then possible if molecules stack as in the $Fe_2Os(CO)_{10}(\mu\text{-}CO)_2$ structure. The overall composite *disordered macrostructure* can now be formed by twinning of these microdomains along the *b* axis.

Either of these (or a combination of the two) is possible. The first requires fewer assumptions (and thus is favored by Occham's razor); the second allows for the additional observation that the O_{12} periphery of $Fe_3(CO)_{10}(\mu\text{-}CO)_2$ does not have a perfect inversion center and that a precise 0.50:0.50 occupancy is therefore not favored. It would be interesting to survey $Fe_3(CO)_{10}(\mu\text{-}CO)_2$ crystals and search for a possible superlattice in their diffraction pattern, particularly at extremely low temperature, where the possibility of intramolecular rearrangement is reduced. We have previously observed one example of a structure with a well-defined subcell but with a diffuse superlattice doubling the axis length in one direction (i.e. $[(Me_6C_6)_3Nb_3Cl_3]Cl$).[10]

Thermal Parameters of the Iron Atoms in $Fe_2Os(CO)_{10}(\mu\text{-}CO)_2$

It is clear from Figures 1 and 2 that iron atoms (but not the osmium atoms) have thermal parameters extended in the *b* direction. Thus, in molecule A, $B_{22}(Fe) = 5.87\text{–}6.28$ Å^2 and $B_{22}(Os) = 2.91$ Å^2; in molecule B, $B_{22}(Fe) = 4.98\text{–}5.41$ Å^2 and $B_{22}(Os) = 2.65$ Å^2. A similar situation also occurs in $Fe_3(CO)_{10}(\mu\text{-}CO)_2$.[2] Here (in different units) β_{22}(Fe, bridged) = 0.0140–0.0162 whereas β_{22}(Fe, nonbridged) = 0.0067.

This latter fact was pointed out to M.R.C. by Dr. B. F. G. Johnson in a private conversation. He regarded it as important evidence for his proposed model for stereochemical nonrigidity of $Fe_3(CO)_{10}(\mu\text{-}CO)_2$ involving the interchange of carbonyl ligands by a C_2 rotation[11] of the Fe_3 triangle as opposed to a C_3 rotation[2,12,13] of the Fe_3 triangle relative to the external carbonyl groups. A recent variable-temperature Mössbauer-effect study on $Fe_3(CO)_{10}(\mu\text{-}CO)_2$[14] has been reported and also indicates that a "low-temperature single-crystal X-ray study of $Fe_3(CO)_{12}$" is being undertaken. The results of this study appear to be inconsistent with either a C_2 or C_3 rotation of the Fe_3 triangle.

Acknowledgment. We thank Professor Jim D. Atwood and Dr. Rasul Shojaie of this department for providing us with crystals of $Fe_2Os(CO)_{10}(\mu\text{-}CO)_2$ and for continued cooperation. We also thank Professor Bruce Foxman (Brandeis University) for providing us with a copy of his version of ORTEP-II for the IBM PC.

Supplementary Material Available: A listing of anisotropic thermal parameters (1 page); a listing of observed and calculated structure factors (29 pages). Ordering information is given on any current masthead page.

---

[10] Churchill, M. R.; Chang, S. W.-Y. *J. Chem. Soc., Chem. Commun.* **1974**, 248.

[11] Johnson, B. F. G. *J. Chem. Soc., Chem. Commun.* **1976**, 703.

[12] Cotton, F. A.; Hunter, D. L. *Inorg. Chim. Acta* **1974**, *11*, L9.

[13] Dorn, H.; Hanson, B. E.; Motell, E. *Inorg. Chim. Acta* **1981**, *54*, L71.

[14] Grandjean, F.; Long, G. J.; Benson, C. G.; Russo, U. *Inorg. Chem.* **1988**, *27*, 1524.